Time integrations in solution of diffusion problems by local integral equations and moving least squares approximation

V. Sladek[1], J. Sladek[1] & Ch. Zhang[2]
[1]*Institute of Construction and Architecture, Slovak Academy of Sciences, Bratislava, Slovakia*
[2]*Department of Civil Engineering, University of Siegen, Germany*

Abstract

The paper deals with the numerical solution of initial-boundary value problems for diffusion equation with variable coefficients by using a local weak formulation and a meshless approximation of spatial variations of the field variable. The time variation is treated either by the Laplace transform technique or by the linear Lagrange interpolation in the time stepping approach. Advanced formulation for local integral equations is employed. A comparative study of numerical results obtained by the Laplace transform and the time stepping approach is given in a test example for which the exact solution is available and utilized as a benchmark solution.
Keywords: transient heat conduction, weak formulation, Laplace transform, time stepping, accuracy, computational efficiency.

1 Introduction

The diffusion and the transient heat conduction problems in functionally graded materials belong to frequent engineering problems. From the mathematical point of view, the solution of initial-boundary value problems for the diffusion equation with variable coefficients is rather complex task and therefore there is a demand to have sophisticated and efficient numerical techniques. The local weak formulations appear to be appropriate. The local integral equations replacing the governing equations are acceptable from the physical point of view, since such equations express the balance principles. The variation of material coefficients is involved naturally without any complication as compared with the formulations


WIT Transactions on Modelling and Simulation, Vol 52,
www.witpress.com, ISSN 1743-355X (on-line)
doi:10.2495/BE110191

for homogeneous media. Furthermore, the local formulation enables us to develop truly meshless formulations and so eliminate all inappropriateness of finite size elements employed in standard element based discretization methods. Besides the advantages of the meshless formulations one should name also their main drawback which consists in prolongation of creation of the discretized system matrix. It is given by the fact that the shape functions in meshless approximations are not given in a closed form and a computational procedure is required for evaluation of the shape functions at each point. Nevertheless this disadvantage can be eliminated by decreasing the amount of the integration points which can be done by performing the integrations analytically [1]. The other disadvantage is the failure of accuracy of higher order derivatives of the shape functions at points near the boundary of the analyzed domain. This can be avoided by expressing such derivatives in terms of the first order derivatives [1].

The other task which should be solved in the case of transient problems is the treatment of the time variable. Besides the well known time stepping approaches, the Laplace transform technique is often used alternatively. In this paper, both these techniques are used in combination with the local integral equation formulation and the MLS approximation in the comparative study for accuracy in a test example.

2 Governing equations and local integral equation formulations

The governing equation for diffusion problems is the same as for transient heat conduction with the absent volume density of heat sources $w(\mathbf{x},t)$. Thus, we shall consider initial-boundary value problems for the partial differential equation [2]

$$\left(\lambda(\mathbf{x})u_{,k}(\mathbf{x},t)\right)_{,k} - \rho(\mathbf{x})c(\mathbf{x})\frac{\partial u(\mathbf{x},t)}{\partial t} = 0 \ , \quad \text{in} \quad \Omega\times[0,T] \tag{1}$$

where $u(\mathbf{x},t)$ can be interpreted as the temperature field. In isotropic and continuously non-homogeneous media, the material parameters, such as the mass density $\rho(\mathbf{x})$, the volume density of the specific heat per unit mass $c(\mathbf{x})$, and the thermal conductivity coefficient $\lambda(\mathbf{x})$ are spatially dependent and the governing equation is the partial differential equation (PDE) of parabolic type with variable coefficients. The first term on the left-hand side of Eq.(1) is the divergence of the heat flux vector

$$q_k(\mathbf{x},t) = -\lambda(\mathbf{x})u_{,k}(\mathbf{x},t) \tag{2}$$

and the second term is the rate of the temporal change of the volumetric density of heat.

Three types of physically reasonable boundary conditions are applicable (Dirichlet b.c., Neumann b.c., and Robin b.c.). The boundary conditions are to be supplemented by the initial condition, which in the present parabolic problem is the initial value of the temperature $u(\mathbf{x},0) = v(\mathbf{x})$ in $\Omega\cup\partial\Omega$.

Since the energy balance should be satisfied in an arbitrary finite part of the continuum Ω^c bounded with the boundary $\partial\Omega^c$, we may write the integral relationship

$$\int_{\partial\Omega^c} n_i(\boldsymbol{\eta})\lambda(\boldsymbol{\eta})u_{,i}(\boldsymbol{\eta},t)d\Gamma(\boldsymbol{\eta}) - \int_{\Omega^c} \rho(\mathbf{x})c(\mathbf{x})\frac{\partial}{\partial t}u(\mathbf{x},t)d\Omega(\mathbf{x}) = 0 \tag{3}$$

It is easy to show that equation (3) is the integral equivalent of the differential governing equation (1).

Sometimes, the Laplace transform (LT) technique is an efficient tool for treatment of the time evolution. Then, the time variable is eliminated temporarily and replaced by the Laplace transform parameter p. The governing equations (1) and/or (3) can be rewritten for the Laplace transform of the temperature as

$$\left(\lambda(\mathbf{x})\overline{u}_{,k}(\mathbf{x},p)\right)_{,k} - p\rho(\mathbf{x})c(\mathbf{x})\overline{u}(\mathbf{x},p) = -\rho(\mathbf{x})c(\mathbf{x})v(\mathbf{x}) \tag{4}$$

$$\int_{\partial\Omega^c} n_i(\boldsymbol{\eta})\lambda(\boldsymbol{\eta})\overline{u}_{,i}(\boldsymbol{\eta},p)d\Gamma(\boldsymbol{\eta}) - p\int_{\Omega^c} \rho(\mathbf{x})c(\mathbf{x})\overline{u}(\mathbf{x},p)d\Omega(\mathbf{x}) = -\int_{\Omega^c} \rho(\mathbf{x})c(\mathbf{x})v(\mathbf{x})d\Omega(\mathbf{x}). \tag{5}$$

The boundary conditions for the Laplace transform of the temperature can be obtained by direct application of the Laplace transformation to the prescribed boundary conditions. In the LT-approach, the numerical inversion of the LT is a key issue, since it is an ill-posed problem. Various Laplace-inversion algorithms are available in literature. Regarding good experience with the Stehfest's algorithm [3], we shall use this algorithm in the present analysis with taking 10 values of the transform parameter for each time instant.

The derived local integral equations (LIE) (3) and/or (5) are the restriction relationships, which should be satisfied together with the prescribed initial and boundary conditions in solving initial-boundary value problems. In order to solve these equations, the spatial variation of field variables is usually approximated in terms of certain shape functions and unknowns related to a finite number of nodal points. Implementation of the spatial approximation in the LIE (3) results in the ordinary differential equations (ODE) for the nodal unknowns which is known as a semi-discrete formulation. On the other hand, having used the spatial approximation in the LIE (5) for certain value of the LT parameter, we obtain a system of algebraic equations for the nodal unknowns of the Laplace transforms of the field variable (temperature).

3 MLS-approximation for spatial variations

Recall that the Moving Least Squares approximation belongs to mesh free approximations since no predefined connectivity among nodal points is required. In this paper, we shall consider the Central Approximation Node (CAN) concept of the MLS-approximation [4].

Let $\mathbf{x}^q$ be the CAN for the approximation at a point $\mathbf{x}$. Then, the amount of nodes involved into the approximation at $\mathbf{x}$ is reduced a-priori from N_t (total number of nodes) to N^q, where N^q is the number of nodes supporting the approximation at the CAN $\mathbf{x}^q$, i.e. the amount of nodes in the set $\mathcal{M}^q = \left\{\forall \mathbf{x}^a;\, w^a(\mathbf{x}^q) > 0\right\}_{a=1}^{N_t}$, where $w^a(\mathbf{x})$ is the weight function associated with the node $\mathbf{x}^a$ at the field point $\mathbf{x}$. In this paper, we employ the Gaussian weights [4]. The MLS-CAN approximation for spatial variation of the field variable $f(\mathbf{x}) \in \{u(\mathbf{x},t), \overline{u}(\mathbf{x},p)\}$ is given by

$$f(\mathbf{x}) \approx \sum_{a=1}^{N^q} \hat{f}^{n(q,a)} \phi^{n(q,a)}(\mathbf{x}), \tag{6}$$

where $n(q,a)$ is the global number of the a-th local node from $\mathcal{M}^q$, $\hat{f}^{n(q,a)} \in \{\hat{u}^{n(q,a)}(t), \hat{\overline{u}}^{n(q,a)}(p)\}$, with $\hat{f}^{n(q,a)}$ being the nodal unknowns, which are different from the nodal values of physical quantities, in general. In this paper, we shall specify the CAN $\mathbf{x}^q$ as the nearest node to the approximation point $\mathbf{x}$. Recall that the shape functions $\phi^m(\mathbf{x})$ are not known in closed form and a computational procedure must run for evaluation at each approximation point $\mathbf{x}$. This is the main handicap of mesh-free approximations as compared with mesh-based approximations utilizing mostly polynomial interpolations.

Besides the approximation of field variables, we need also their gradients which can be approximated as gradients of approximated fields (6)

$$f_{,j}(\mathbf{x}) \approx \sum_{a=1}^{N^q} \hat{f}^{n(q,a)} \phi_{,j}^{n(q,a)}(\mathbf{x}) \tag{7}$$

and similarly, one can approximate also higher-order derivatives. Recall that the evaluation of the derivatives of the shape functions is still more complicated than the evaluation of shape functions and also the accuracy of such approximations is worse.

Substituting these approximations into the governing equation (5) considered at nodal points $\mathbf{x}^c$ ($\Omega^c \ni \mathbf{x}^c$ is a sub-domain around the node $\mathbf{x}^c$), one obtains the system of algebraic equations

$$\sum_g \left(K^{cg} - p_n M^{cg}\right) \hat{\overline{u}}^g(p_n) = -\overline{R}^c(p_n), \quad (c = 1,2,...,N_t),\ (n = 1,2,...,N) \tag{8}$$

where the matrix elements are given as

$$K^{cg} = \int_{\partial\Omega^c} n_i(\boldsymbol{\eta}) \lambda(\boldsymbol{\eta}) \phi_{,i}^{n(q_\eta,a)}(\boldsymbol{\eta}) d\Gamma(\boldsymbol{\eta}), \quad M^{cg} = \int_{\Omega^c} \rho(\mathbf{x}) c(\mathbf{x}) \phi^{n(q_x,a)}(\mathbf{x}) d\Omega(\mathbf{x}),$$

$$\overline{R}^c(p_n) = \int_{\Omega^c} \rho(\mathbf{x})c(\mathbf{x})v(\mathbf{x})d\Omega(\mathbf{x}), \tag{9}$$

with g being global numbers of nodes generated by $n(q_\eta, a)$ and/or $n(q_x, a)$, where q_x is the nearest nodal point to the integration point $\mathbf{x}$.

Similarly, substituting the approximations for the temperature and its gradients into the governing equation (3), we obtain the system of the ODE

$$\sum_g \left(K^{cg}\hat{u}^g(t) - M^{cg}\frac{\partial \hat{u}^g(t)}{\partial t} \right) = 0, \qquad (c = 1, 2, ..., N_t). \tag{10}$$

The integrations in the integrals defined in Eqn. (9) can be performed analytically by using the Taylor series expansions for the material coefficients and the shape functions [1]. For this purpose the circular shape is chosen for sub-domains and their radius should be sufficiently small to restrict the order for the derivatives of shape functions.

In order to solve the ODE (11), we employ a polynomial interpolation for the time variation of the nodal unknowns.

4 Linear time interpolations (LLI)

Let us split the time interval $[0, T]$ by discrete time instants t_i into a finite number of subintervals $[t_i, t_{i+1}]$ to complete the discretization in the semi-discrete formulation. In the case of Linear Lagrange Interpolation (LLI) the element T_i is defined as the interval $T_i = [t_i, t_{i+1}]$ with the interior points being parametrized as

$$t\big|_{T_i} = \sum_{a=1}^{2} t_{i-1+a}N^a(\tau) = t_i + \frac{\Delta t_i}{2}(1+\tau), \qquad \tau \in [-1, 1] \tag{11}$$

since $N^1(\tau) = (1-\tau)/2$, $N^2(\tau) = (1+\tau)/2$. The time dependence of a physical variable $u(t)$ is approximated on T_i by the interpolation

$$u(t)\big|_{T_i} = \sum_{a=1}^{2} u_{i-1+a}N^a(\tau) = \frac{1}{2}(u_{i+1} + u_i) + \frac{\tau}{2}(u_{i+1} - u_i), \qquad u_k = u(t_k). \tag{12}$$

Then, the time derivative $\dot{u}(t) = du(t)/dt$ is approximated by the constant

$$\dot{u}(t)\big|_{T_i} = \frac{1}{J(\tau)}\frac{du}{d\tau}\bigg|_{T_i} = \frac{1}{\Delta t_i}(u_{i+1} - u_i), \tag{13}$$

since the Jacobian of the transformation (11) is given as $J(\tau) = dt/d\tau\big|_{T_i} = \Delta t_i/2$.

Making use a different parametrization $\theta = (1+\tau)/2$ with $\theta \in [0,1]$, we obtain from (12) and (13)

$$u(t_i + \theta\Delta t_i) = \theta u_{i+1} + (1-\theta)u_i, \quad \dot{u}(t_i + \theta\Delta t_i) = (u_{i+1} - u_i)/\Delta t_i \tag{14}$$

Considering the system of the ODE (11) at $t = t_i + \theta\Delta t_i$, we obtain

$$\sum_g \left(K^{cg} - \frac{1}{\theta\Delta t_i} M^{cg} \right) \hat{u}^g_{i+1} = \sum_g \left((1 - \frac{1}{\theta}) K^{cg} - \frac{1}{\theta\Delta t_i} M^{cg} \right) \hat{u}^g_i \ , \ (i = 0,1,2,...) \quad (15)$$

which is the well known θ-method used in time stepping approaches for solution of the ODE with $\theta \in (0,1]$.

5 Numerical tests

In our numerical experiments, it is important to have the exact solution which could be used as a benchmark solution. In this paper, we consider a square domain $L \times L$ occupied by medium with exponentially graded heat conduction as well as specific heat while constant mass density: $\rho = \text{const}$., $\lambda(\mathbf{x}) = \lambda_0 \exp(2\delta x_2 L) = c(\mathbf{x})\lambda_0 / c_0$. If constant values of the temperature are prescribed on the bottom u_0 and top u_L of the square, while the lateral sides are thermally insulated for $t \in [0, T]$ and constant initial value of temperature $v(\mathbf{x}) = \text{const} = v$ is assumed, the exact solution is available [5]. In numerical computations, we have used $\lambda_0 = 1 = c_0 = \rho$, $\delta = 1$, $u_0 = 1 = v$, $u_L = 20$. The uniform distribution of nodal points is employed with h being the distance between two neighbour nodes. Furthermore, in the MLS-approximation we have used quadratic polynomials as the basis functions, Gaussian weights with the shape factor $c = h$, radius of the influence domain $R_i = 3.001 \times h$, and the radius of circular sub-domains Ω^c in the local weak formulation is $r^c = 0.3 \times h$. In the analytical integrations of the LIE, we have used the third order of the derivatives of the shape functions as maximal and the Taylor series expansions of the integrands have been stopped on the 8th power of the radius of sub-domain.

It can be seen from Fig. 1 that considerable errors are sharply localized in both the space and time for short time steps. The inaccuracy of the numerical results by the LLI approach is partially decreased and remarkably delocalized with increasing the time step, while in the case of LT approach the delocalization is marginal as compared to the substantial increase of accuracy. For more detailed study of errors near the top side of the analyzed domain, we have used 1296 nodes and the test point is $(L/2,\ 0.9L)$.

Fig. 2 shows the numerical results at the point (x_1, x_2) which is the nearest node to the point $(L/2,\ 0.9L)$. The sequences of time instants at which the numerical results are received are given as follows: $t_i = 4 \times 10^{-4} + (i-1)\Delta t$, $(i = 1,2,....)$ for three different time steps Δt. Thus, the time step is used for specification of time instants in the calculations by both the LT approach and LLI approach, but in the latter one, the time step is also the length of the time interval within which the interpolation is assumed.

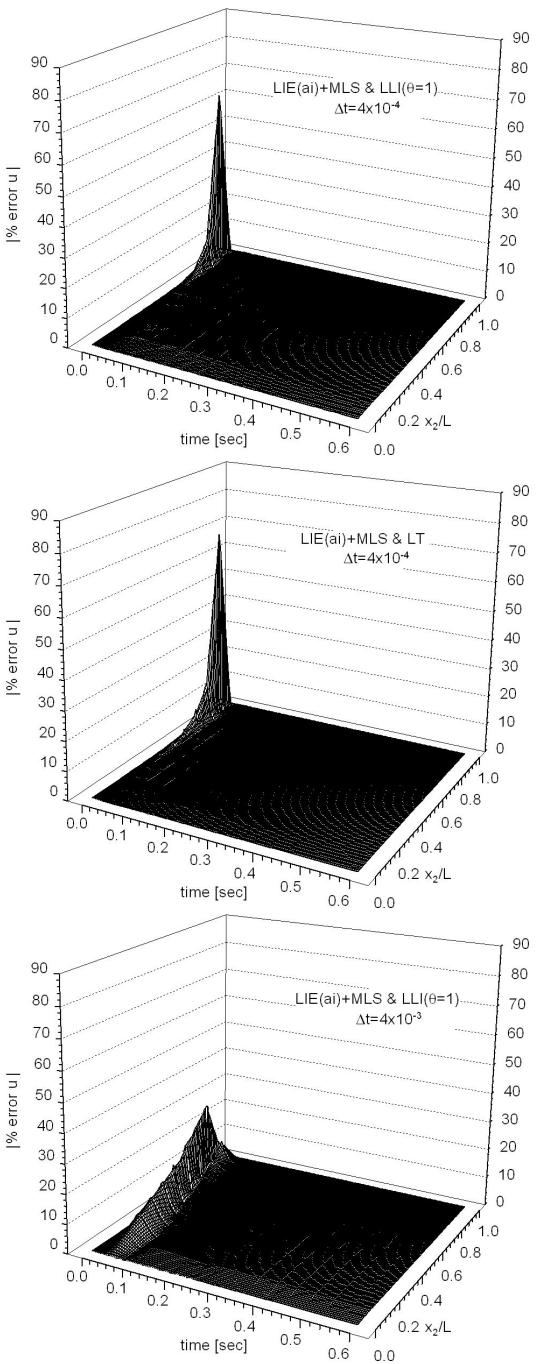

Figure 1: Evolutions of error distributions by LLI and LT approaches using 121 nodes and various time steps Δt.

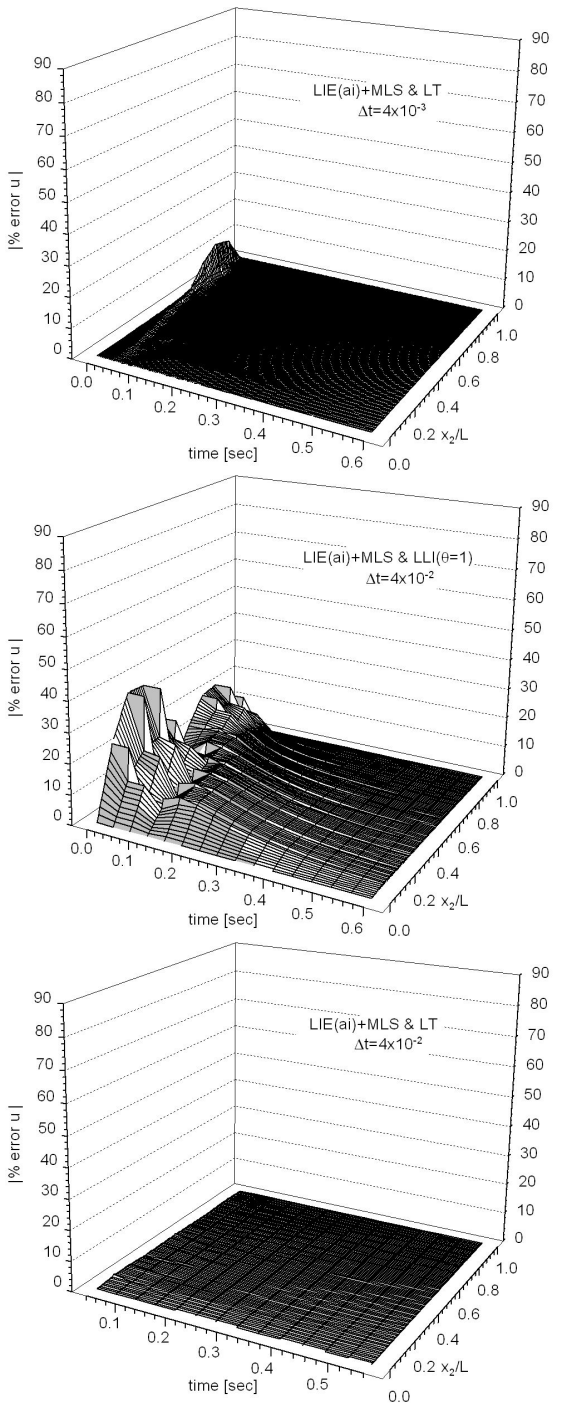

Figure 1: Continued.

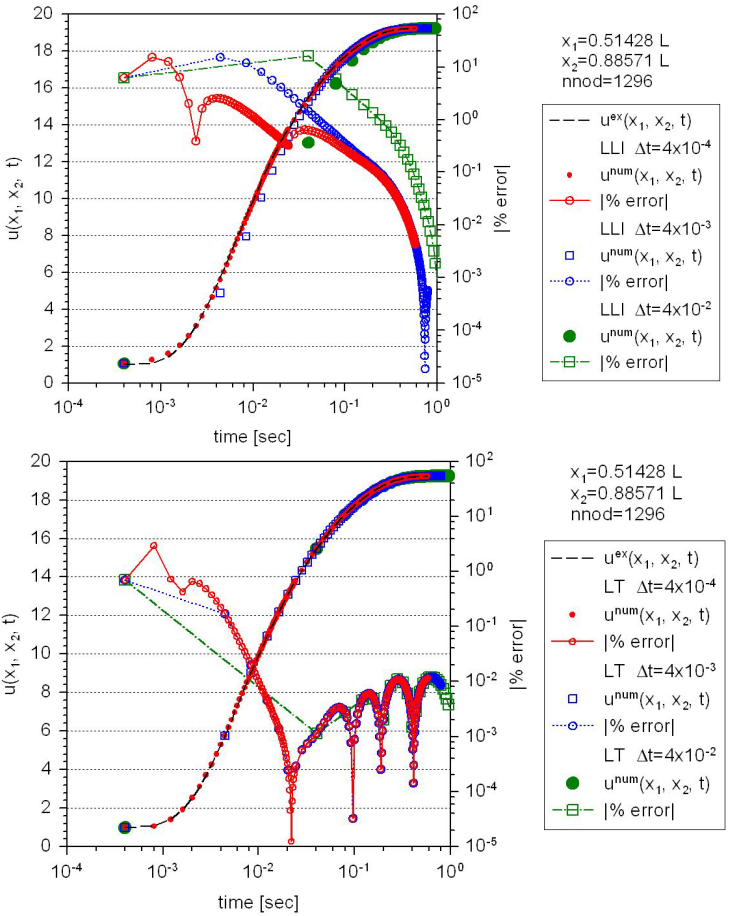

Figure 2: Time evolutions of the computed temperature and its accuracy by the LLI and LT approaches at the selected point (x_1, x_2) using 1296 nodes and three various lengths of time steps.

Recall that the prescribed boundary temperature $u_L = 20$ represents a sudden change at $t = 0$ with respect to the initial value of temperature $v = 1 = u_0$. It can be seen that better accuracy is achieved by the LT approach especially when the longer time steps are employed.

Note that three characteristic lengths play a role in this fully discretized transient field problem:

(i) $l_h = h$ represents the distance between two neighbouring nodes

(ii) $l_S = R_i h$ represents the radius of the influence domain which is used for selection of nodes contributing to the meshless approximation at certain point

(iii) $l_T = \sqrt{(\lambda / \rho c)\Delta t}$ is the characteristic length corresponding to the time step Δt and represents the horizon reached by the heat conduction during the time step with respect to certain point. In time stepping techniques, the optimal choice is $l_T \approx h$, because information at previous time instant t_{i-1} cannot reach the nearest neighbour node at t_i, if $l_T < h$; on the other hand, if $l_T > h$, information at a node from the nearest neighbour node is not fresh.

Now, we can explain the inaccuracy of numerical results by both the LLI and LT approaches at several early time instants $t_i = i\Delta t$ $(i = 1, 2, ..., 5)$ if $\Delta t = 4 \times 10^{-4}$. In this case $l_T = 2 \times 10^{-2}$, hence the choice of 1296 uniformly distributed nodes is almost optimal. Then, $h = 1/(\sqrt{1296} - 1) = 0.02857$ and at early time instants, the prescribed boundary value $u_L = 20$ (which is different from the initial value $v = 1$) affects the approximation in the boundary layer $L - (l_T + l_S) < x_2 < L$ and hence also in the boundary layer $L - (l_T + l_S) < x_2 < L - l_T$, i.e. at points which lie behind the horizon of the heat conduction from the top of the analyzed domain. Quite different is the situation near the bottom of the analyzed domain, where the prescribed boundary value of the temperature is the same as its initial value $u_0 = v = 1$. With increasing Δt, l_T is increased and hence not only the time interval but also the boundary layer of inaccurate results by the time stepping approaches become wider.

On the other hand, in the case of the LT approach the solution at a time instant is independent of the time step and therefore the accuracy at the time instants $t_i = 4 \times 10^{-4} + (i-1)\Delta t_2$ (which occurs after $(i-1)$ steps $\Delta t_2 = 4 \times 10^{-2}$) is the same as the accuracy after $10 \times (i-1)$ steps $\Delta t_3 = 4 \times 10^{-3}$ and/or after $100 \times (i-1)$ steps $\Delta t_4 = 4 \times 10^{-4}$. These conclusions are confirmed by the numerical results presented in Fig.2 and also in Fig.3.

The results in Fig.3 confirm the spatial delocalization of the error with increasing the size of the time step. In the case of the LT approach, this delocalization is suppressed by decrease of the maximum value of the error.

6 Conclusions

The local weak formulation is proposed for solution of transient heat conduction in FGM. The spatial variation of temperature is approximated by using the MLS approximation, while the time dependence is treated either by the Laplace transform or by the linear Lagrange interpolation in the time stepping method. Both the LT and LLI approaches can give results with reasonable accuracy except very early time instants after sudden change of initial values by different

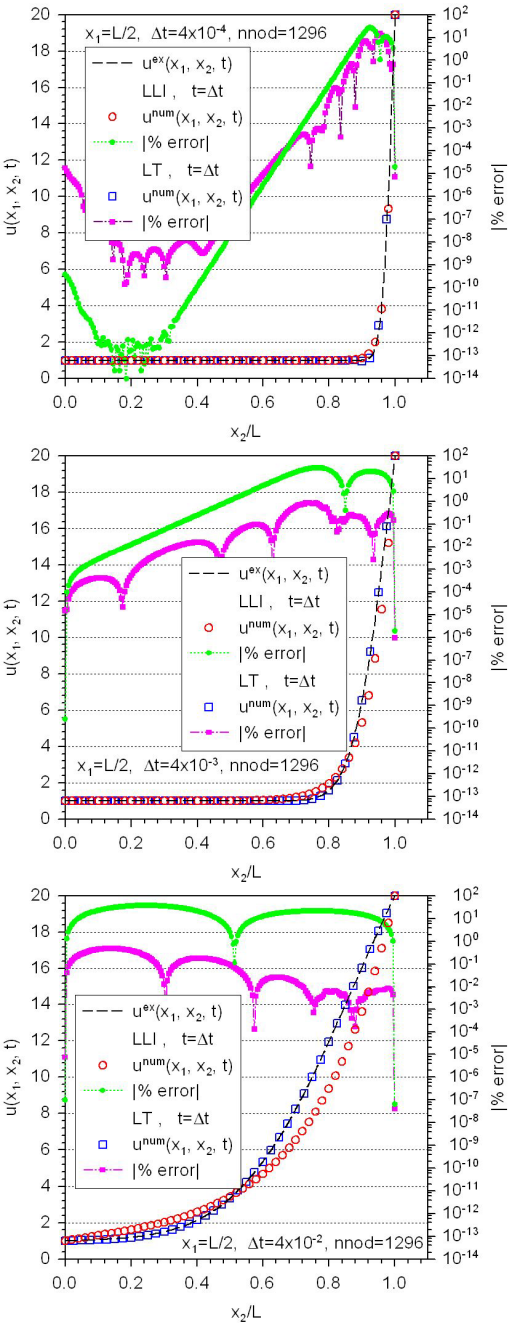

Figure 3: Spatial distributions of the temperatures and their accuracies by the LLI and LT approaches at the time instant $t = \Delta t$ for three values of the time steps Δt.

prescribed boundary values. The time stepping approach is sensitive to the choice of the time step, while the LT approach is stable. On the other hand, the computational economy is better in time stepping approaches than in the LT approach if the solution is required not only at few time instants but within a time interval.

Acknowledgements

This article has been produced with the financial assistance of the European Regional Development Fund (ERDF) under the Operational Programme Research and Development/Measure 4.1 Support of networks of excellence in research and development as the pillars of regional development and support to international cooperation in Bratislava region/Project No. 26240120020 Building the centre of excellence for research and development of structural composite materials – 2nd stage.

This work has been partially supported by the Slovak Science and Technology Assistance Agency registered under number APVV-0032-10, the Slovak Grant Agency VEGA-2/0039/09 and the German Research Foundation (DFG, ZH 15/14-1), which are gratefully acknowledged

References

[1] Sladek V., Sladek J., Local integral equations implemented by MLS-approximation and analytical integrations. *Engineering Analysis with Boundary Elements* **34**, pp. 904-913, 2010.

[2] Wrobel L.C, The Boundary Element Method, Vol1: Applications in Thermo-Fluids and Acoustics, Wiley: Chichester, 2002.

[3] Stehfest H., Algorithm 368: numerical inversion of Laplace transform. *Communication of the Association for Computing Machinery*, **13**, pp. 47-49; 624, 1970.

[4] Sladek V., Sladek J., Zhang Ch., Computation of stresses in non-homogeneous elastic solids by local integral equation method: a comparative study. *Computational Mechanics* 41, pp. 827-845, 2008.

[5] Sladek V., Sladek J., Tanaka M., Zhang Ch., Transient heat conduction in anisotropic and functionally graded media by local integral equations. *Engineering Analysis with Boundary Elements* **29**, pp. 1047-1065, 2005.